

THERMODYNAMIC ASSESSMENT OF COMBINED SUPERCRITICAL CO₂ (SCO₂) AND ORGANIC RANKINE CYCLE (ORC) SYSTEMS FOR CONCENTRATED SOLAR POWER

Jian Song*, Michael Simpson, Kai Wang, Christos N. Markides

Clean Energy Processes (CEP) Laboratory, Department of Chemical Engineering, Imperial College London, London SW7 2AZ, UK

*Corresponding Author. Email: jian.song@imperial.ac.uk

ABSTRACT

Concentrated solar power (CSP) systems are acknowledged as a promising technology for solar energy utilisation. Supercritical CO₂ (SCO₂) cycle systems have emerged as an attractive option for power generation in CSP applications due to the favourable properties of CO₂ as a working fluid. In order to further improve the overall performance of such systems, organic Rankine cycle (ORC) systems can be used in bottoming-cycle configuration to recover the residual heat. This paper presents a thermodynamic performance assessment of a combined SCO₂/ORC system in a CSP application using parabolic-trough collectors. The parametric analysis indicates that the heat transfer fluid (HTF) temperature at the inlet of the cold tank, and the corresponding HTF mass flow rate, have a significant influence on the overall system performance. The results suggest that the combined system can offer significant thermodynamic advantages at progressively lower temperatures. Annual simulations for a case study in Seville (Spain) show that, based on an installation area of 10,000 m², the proposed combined cycle system could deliver an annual net electricity output of 2,680 MWh when the HTF temperature at the cold tank inlet is set to 250 °C, which is 3% higher than that of a stand-alone CO₂ cycle system under the same conditions. Taking the size of the thermal storage tanks into consideration, a lower HTF temperature at the cold tank inlet and a lower mass flow rate would be desirable, and the combined system offers up to 66% more power than the stand-alone version when the HTF inlet temperature is 100 °C.

Keywords: CSP, combined cycle, SCO₂ cycle, ORC, performance assessment

NOMENCLATURE

Abbreviations

CSP	concentrated solar power
HTF	heat transfer fluid
ORC	organic Rankine cycle
SCO ₂	supercritical CO ₂

Symbols

T	temperature (K)
s	specific entropy (J/kg·K)
W_n	net power output (W)

1. INTRODUCTION

As a ubiquitous and accessible heat source, solar energy is widely recognised as having the potential to play an important role in clean power generation [1-3]. Concentrated solar power (CSP) systems have appeared as an effective solution for solar energy utilisation and permit the use of thermal-energy storage at low costs relative to electrical-energy storage [4]. Consequently, various power-cycle options for CSP applications have received growing attention in recent years [5,6]. Amongst the existing technologies, supercritical CO₂ (SCO₂) cycle systems have emerged as a promising heat-to-power conversion technology thanks to the key advantages offered by the properties of CO₂ as a working fluid [7,8]. In addition, a better temperature match can be obtained between the heat source and the power cycle thereby reducing the exergy loss in the heat exchange processes. Beyond CSP applications, fossil fuel [9], nuclear [10], geothermal [11] and waste heat recovery [12] are all potential application areas for SCO₂-cycle systems.

The pressure ratio of SCO_2 cycles is generally small, and the turbine outlet temperature would be relatively high. A recuperator is typically installed to utilise the energy of the hot stream from the turbine but the residual heat which is dissipated in the pre-cooler remains significant. Although an acceptable efficiency can be attained by CSP- SCO_2 cycle systems, this observation helps to motivate the pursuit of further performance improvements to the overall system, by means of a bottoming cycle used to recover heat from the topping SCO_2 cycle [13].

In this context, organic Rankine cycle (ORC) systems offer an attractive option as they have been proven to be an efficient technology for heat-to-power conversion for low- and medium-temperature and small-to-medium scale applications [14,15]. Besarati and Goswami [16] compared the performance of power systems based on various SCO_2 cycles with bottoming ORCs using different working fluids. Their results indicated that the combined recompression SCO_2 /ORC systems had higher thermal efficiencies, and butane and cis-butene were found to be most appropriate for the bottoming ORC. Similar work was conducted by Padilla et al. [17], whose results revealed that a recompression cycle with main compression intercooling delivered the best thermal performance. Singh and Mishra [18] conducted a performance analysis of combined-cycle power plants driven by solar parabolic-trough collectors; R407c was found to deliver the highest thermal efficiency of 42% in this case. Furthermore, Chacartegui et al. [19] studied simple SCO_2 /ORC combined cycles and several organic working fluids were tested for use in the bottoming cycle,

with results demonstrating that the efficiency of the simple SCO_2 cycle could be increased by 7-12%.

Most previous research has focused on working fluid selection and parameter optimisation of the bottoming ORC system, while limited attention has been paid to the interplay between the topping and bottoming cycles. In addition, overall system analysis and annual performance assessment has been limited, despite being essential for technical evaluation. This paper presents a comprehensive model including sub-models of the solar field and the combined-cycle system, to allow detailed thermodynamic assessments. A case study in Seville (Spain) using the proposed CSP-combined SCO_2 /ORC system is conducted. The two cycles interact via the heat transfer fluid (HTF) temperature at the cold tank inlet (see Fig. 1), motivating an investigation into the influence of this parameter on the system performance. An annual performance evaluation of the overall system is performed to demonstrate the potential of exploiting this kind of combined-cycle CSP systems in practical applications.

2. SYSTEM DESCRIPTION

2.1 CSP - combined SCO_2 /ORC system architecture

A schematic diagram of the CSP-combined SCO_2 /ORC system is shown in Fig. 1, in which the red line (hot) and blue line (cold) represent the HTF loop that absorbs solar energy from the parabolic-trough collectors and transfers heat to the power cycle systems, while the lines coloured in orange and black denote the SCO_2 cycle and the ORC, respectively. The two sub-systems are coupled

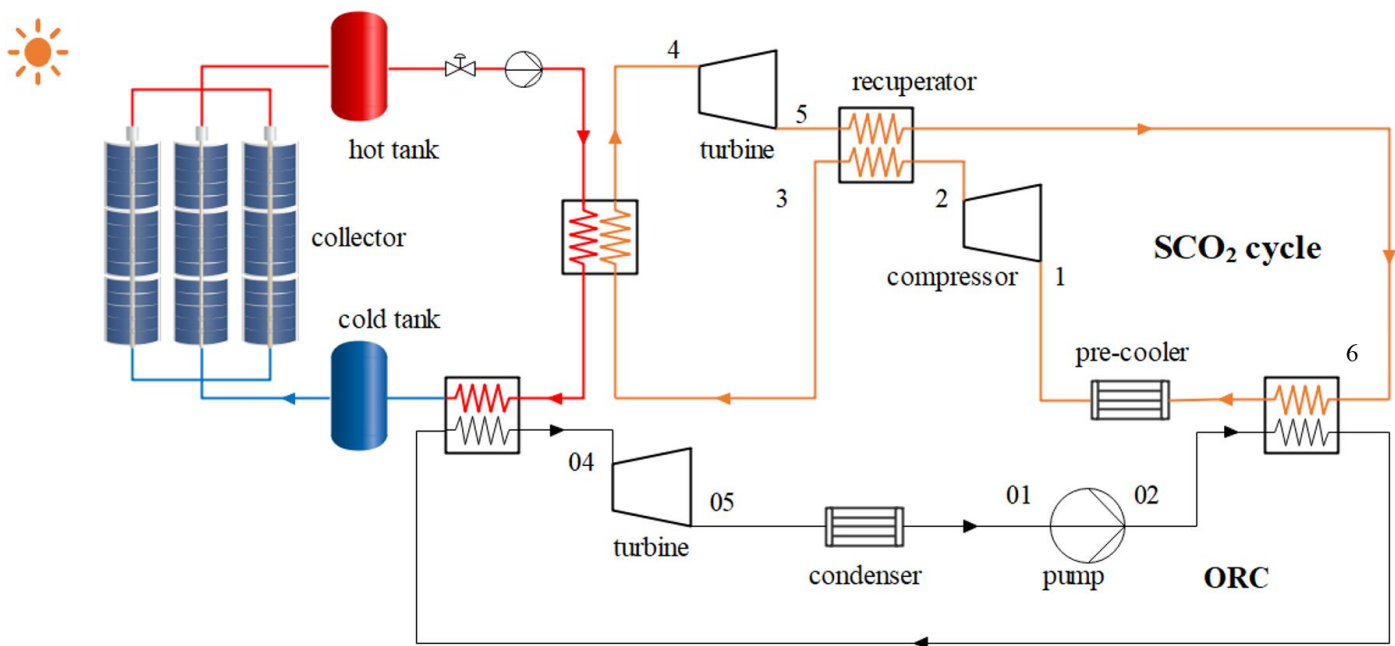


Figure 1. Schematic diagram of CSP-combined SCO_2 /ORC system.

via a shared heat exchanger, which allows the bottoming ORC system to recover the residual heat from the topping cycle system. A T - s diagram of the proposed combined SCO_2/ORC system is shown in Fig. 2.

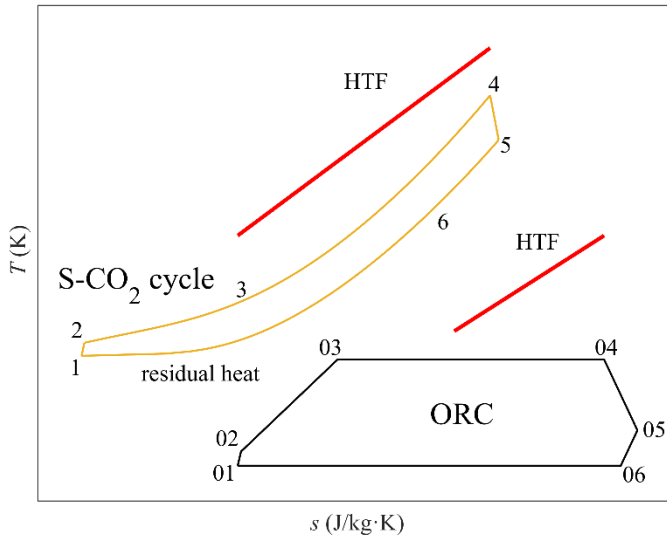


Figure 2. T - s diagram of combined SCO_2/ORC system.

The thermal energy collected by the parabolic-trough collector field is removed by the HTF, which is one of the critical components for storing and transferring thermal energy [20]. Two tanks are used for thermal-energy storage [21,22], in order to overcome the inherent intermittency of the solar resource and to extend the system operating time when the solar irradiance alone is insufficient.

In the topping SCO_2 -cycle system, CO_2 is compressed by the compressor and flows to the recuperator which utilises heat recovered from the hot stream returning from the turbine for pre-heating. The working fluid is heated further by the HTF, expands in the turbine to produce power, and then enters the recuperator, the shared heat exchanger and the pre-cooler for cooling before returning to the compressor, thus completing the cycle.

In the bottoming ORC system, the organic working fluid is first pressurised by the pump, and then heated by the residual heat from the topping SCO_2 -cycle system and the remaining (low-temperature) heat from the HTF. The second heat exchanger is needed to ensure that the HTF is cooled down to the specific temperature required by the cold tank. The ORC evaporation temperature is optimised by sizing the shared heat exchanger and adjusting the heat transferred between the two cycles [23]. Afterwards, the organic vapour expands in the turbine to produce power and then enters the condenser to be cooled and condensed.

2.2 Comprehensive model

The comprehensive model presented in this paper consists of the solar collector, the storage tank and the two power cycle sub-models. A detailed model of the solar field can be found in the authors' previous work [24], and detailed models of both the SCO_2 -cycle system and the ORC system can be found in Ref. [25].

2.3 Conditions and assumptions

The main parameters of the combined-cycle system are summarised in Table 1. The evaporation temperature of the bottoming ORC is optimised by sizing the shared heat exchanger to achieve the maximum net power output using the MATLAB's *fmincon* function.

Table 1. Main parameters of combined SCO_2/ORC system for CSP applications.

Topping SCO_2 cycle system	
Minimum temperature (compressor inlet)	32 °C
Minimum pressure (compressor inlet)	7.8 MPa
Maximum pressure (turbine inlet)	20 MPa
Pinch point temperature difference	6 °C
Compressor efficiency	0.80
Turbine efficiency	0.80
Generator efficiency	0.95
Bottoming ORC system	
Working fluid	R245fa
Condensation temperature	25 °C
Pinch point temperature difference	6 °C
Compressor efficiency	0.80
Turbine efficiency	0.80
Generator efficiency	0.95

3. RESULTS AND DISCUSSION

3.1 Parametric analysis

A case study in Seville (latitude: 37.39°, longitude: -5.99°), Spain, is performed for the proposed CSP-combined SCO_2/ORC system. A collector array with a total area of 10,000 m^2 is selected, which corresponds to the size of typical small-scale solar power plants [26]. The two energy storage tanks (hot and cold, see Fig. 1) are sized to allow continuous operation of the plant for up to 5 hours. The HTF temperature at the cold tank inlet (after transferring heat to the SCO_2/ORC systems) is varied to evaluate its influence on the overall system and the interplay between the two subsystems, while the HTF temperature at the hot tank inlet (after absorbing heat from solar collectors) is set to 400 °C by adjusting the HTF mass flow rate through the valve located on the loop.

For a specified HTF temperature at the cold tank inlet, a lower HTF mass flow rate corresponds to a smaller size of the tank, which would however restrict the solar energy absorption and the solar field thermal efficiency when the tank is filled with HTF. Consequently, there exists an optimal mass flow rate for the solar collection loop to achieve the highest thermal efficiency, beyond which the solar field thermal efficiency no longer increases with increasing HTF mass flow rate. Figure 3 shows that the optimal HTF mass flow rate increases from 8.5 kg/s to 14.0 kg/s when the cold tank inlet temperature is raised from 100 °C to 250 °C.

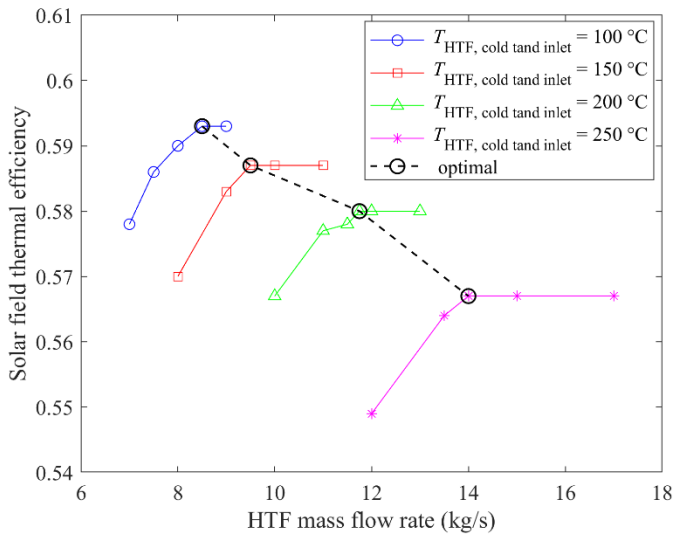


Figure 3. Variation of the solar field thermal efficiency with HTF mass flowrate under different conditions.

In order to avoid fluctuations in the power generated by the system during changeable weather conditions, the thermal-energy storage tanks can be used to maintain the HTF outlet temperature within the range of 360 °C to 400 °C, which ensures that the system operates under relatively stable conditions. A steady-state case with a HTF temperature at the hot tank outlet set to 380 °C is selected in order to evaluate the influence of the cold tank inlet temperature, which ranges from 100 °C to 250 °C, on the combined-cycle system performance and the coupling between the topping and bottoming cycles.

Figure 4 shows that as the HTF temperature at the cold tank inlet increases, the net power output of the bottoming ORC system decreases while that of the topping SCO_2 -cycle system increases at first and then decreases when the temperature exceeds 200 °C. When the HTF temperature at the cold tank inlet is set at 150 °C or lower, there is considerable thermal energy remaining in the HTF for the ORC system to exploit after the topping SCO_2 -cycle system has extracted its heat input. This leads

to a high power output from the ORC system. In contrast, when the HTF temperature at the cold tank inlet is set to be 200 °C or higher, the ORC system only recovers the residual heat from the topping-cycle system. The performance improvement to the SCO_2 -cycle system from the bottoming ORC system is therefore limited in this case, and only accounts for a 3% increase. A HTF temperature at the cold tank inlet of 200 °C is optimal for the combined-cycle system to deliver the maximum net power output of 1,190 kW. However, this high temperature is also associated with a large HTF mass flow rate (see Fig. 3), since the total area of the solar collector and the HTF temperature at hot tank inlet are kept constant. The tank volumes required are therefore also large, and it is expected that this would also lead to an escalation of costs. The thermo-economic trade-off is therefore worth taking into consideration in future work to assess the performance of the combined system.

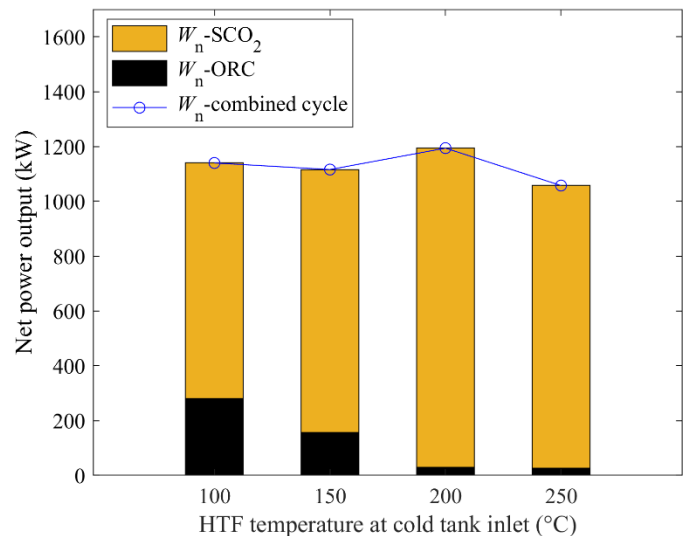


Figure 4. Net power output of the proposed CSP-combined SCO_2 /ORC system under different conditions of the HTF temperature at the cold tank inlet.

3.2 Annual performance evaluation

Annual performance evaluations of the CSP-combined SCO_2 /ORC system are implemented using local weather data comprised of hourly solar irradiance and air temperature data in Seville, Spain. The four aforementioned cases, in terms of the HTF temperature at the inlet of the cold tank (100 °C, 150 °C, 200 °C and 250 °C, see Fig. 3 and Fig. 4) and corresponding optimal mass flowrates presented in Section 3.1 are selected for the assessment.

Figure 5 shows the annual electricity output of the proposed combined system and a comparison to that generated by a stand-alone SCO_2 -cycle system under the

same condition. Performance improvements can be achieved by including the bottoming ORC system, especially under the conditions that correspond to low HTF inlet temperatures. This is because in the stand-alone SCO_2 -cycle system, the recuperation process is restricted when the HTF cold tank return temperature is low, whereas in the combined-cycle system, the recuperation of the topping SCO_2 cycle is still sufficient as the residual heat from HTF (the low-temperature portion) can be recovered by the bottoming ORC system, which additionally raises the ORC evaporation temperature to achieve higher thermal efficiencies.

The maximum performance improvement on the stand-alone CO_2 cycle system reaches 66% at the lowest HTF temperature of 100 °C. As mentioned above, this low temperature and the corresponding small HTF mass flowrate is preferable from the thermal storage size and cost perspectives. When the HTF temperature is raised to 250 °C, the CSP-combined SCO_2 /ORC system delivers the maximum electricity output of 2,680 MWh, which is still 3% higher than that of the stand-alone SCO_2 -cycle system, though the bottoming ORC is mainly for residual heat recovery from the topping SCO_2 cycle in this case.

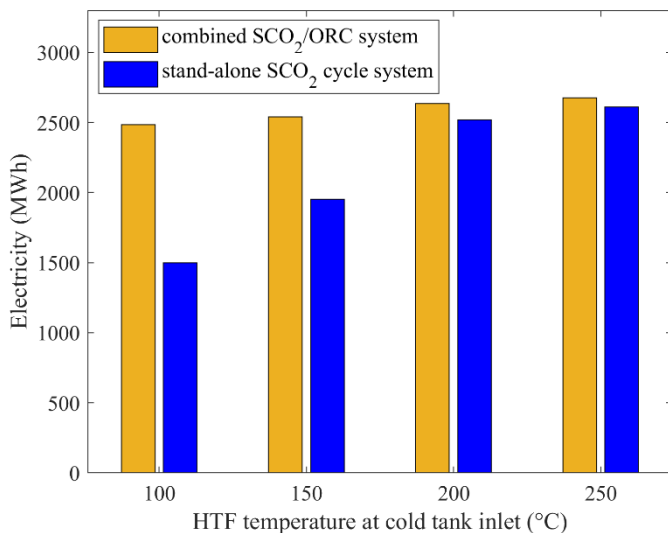


Figure 5. Annual performance evaluation of CSP-combined SCO_2 /ORC system and CSP- SCO_2 cycle system.

4. CONCLUSIONS

Combined SCO_2 /ORC systems offer an attractive option for power generation in CSP applications. A comprehensive model of a CSP-combined SCO_2 /ORC system is presented in this paper and thermodynamic assessments are implemented based on this model.

A lower HTF temperature at the cold tank inlet enables the bottoming ORC system to yield a better thermal performance and allows a corresponding

smaller mass flowrate that is preferable in terms of allowing a smaller thermal store and reducing the associated costs. Although a high HTF temperature is optimal for the combined-cycle system from a pure thermodynamic perspective, a thermo-economic trade-off needs to be taken into consideration and this is highlighted here as an important area for future work.

Annual performance evaluations of the proposed combined-cycle CSP plant based on the real weather data in Seville, Spain, reveal that the system can generate a maximum electricity output of 2,680 MWh at a HTF temperature of 250 °C, which is 3% higher than that of a corresponding, stand-alone SCO_2 -cycle system. However, a maximum performance benefit of 66% more power is demonstrated at the lowest HTF temperature of 100 °C at the inlet of the cold tank. These results demonstrate a promising potential for exploiting this kind of combined-cycle systems for CSP and other similar applications.

ACKNOWLEDGEMENT

This paper was presented at the 11th Int. Conf. on Applied Energy (ICAE2019), 12-15 August 2019, Västerås, Sweden. This work was supported by the UK Engineering and Physical Sciences Research Council [grant number EP/P004709/1] and the Department for International Development (DFID) through the Royal Society-DFID Africa Capacity Building Initiative. The authors would also like to thank the Zijing Scholarship awarded by Tsinghua University to Jian Song in support of this research. Data supporting this publication can be obtained on request from cep-lab@imperial.ac.uk.

REFERENCE

- [1] Herrando M, Pantaleo AM, Wang K, Markides CN. Solar combined cooling, heating and power systems based on hybrid PVT, PV or solar-thermal collectors for building applications. *Renew. Energy* 2019;143:637-47.
- [2] Herrando M, Ramos A, Freeman J, Zabalza I, Markides CN. Technoeconomic modelling and optimisation of solar combined heat and power systems based on flat-box PVT collectors for domestic applications. *Energy Convers. Manag.* 2018;175:67-85.
- [3] Freeman J, Hellgardt K, Markides CN. An assessment of solar-powered organic Rankine cycle systems for combined heating and power in UK domestic applications. *Appl. Energy* 2015;138:605-20.
- [4] Islam MT, Huda N, Abdullah AB, Saidur R. A comprehensive review of state-of-the-art concentrating solar power (CSP) technologies:

- Current status and research trends. *Renew. Sust. Energy Rev.* 2018;91:987-1018.
- [5] Chen Y, Lundqvist P, Johansson A, Platell P. A comparative study of the carbon dioxide transcritical power cycle compared with an organic Rankine cycle with R123 as working fluid in waste heat recovery. *Appl. Therm. Eng.* 2006;26:2142-7.
- [6] Dunham MT, Iverson BD. High-efficiency thermodynamic power cycles for concentrated solar power systems. *Renew. Sust. Energy Rev.* 2014;30:758-70.
- [7] Turchi CS, Ma Z, Neises TW, Wagner MJ. Thermodynamic study of advanced supercritical carbon dioxide power cycles for concentrating solar power systems. *J. Sol. Energy* 2013;135:1-7.
- [8] Song J, Li XS, Ren XD, Gu CW. Performance improvement of a preheating supercritical CO₂ (S-CO₂) cycle based system for engine waste heat recovery. *Energy Convers. Manag.* 2018;161:225-33.
- [9] Mecheri M, Le Moullec Y. Supercritical CO₂ Brayton cycles for coal-fired power plants. *Energy* 2016;103:758-71.
- [10] Ahn Y, Bae SJ, Kim M, Cho SK, Baik S, Lee JI, Cha JE. Review of supercritical CO₂ power cycle technology and current status of research and development. *Nucl. Eng. Technol.* 2015;47:647-61.
- [11] Ahmadi MH, Mehrpooya M, Pourfayaz F. Exergoeconomic analysis and multi objective optimization of performance of a Carbon dioxide power cycle driven by geothermal energy with liquefied natural gas as its heat sink. *Energy Convers. Manag.* 2016;119:422-34.
- [12] Kim YM, Kim CG, Favrat D. Transcritical or supercritical CO₂ cycles using both low-and high-temperature heat sources. *Energy* 2012;43:402-15.
- [13] Li MJ, Zhu HH, Guo JQ, Wang K, Tao WQ. The development technology and applications of supercritical CO₂ power cycle in nuclear energy, solar energy and other energy industries. *Appl. Therm. Eng.* 2017;126:255-75.
- [14] Markides CN. Low-concentration solar-power systems based on organic Rankine cycles for distributed-scale applications: Overview and further developments. *Front. Energy Res.* 2015;3:47.
- [15] Oyewunmi O, Lecompte S, De Paepe M, Markides CN. Thermodynamic optimization of recuperative sub-and transcritical organic rankine cycle systems. In *Proc: 32nd Int. Conf. Effic. Cost Optim. Simul. Environ. Impact Energy Syst., San Diego, 2017.*
- [16] Besarati SM, Goswami DY. Analysis of advanced supercritical carbon dioxide power cycles with a bottoming cycle for concentrating solar power applications. *J. Sol. Energy* 2014;136:010904.
- [17] Padilla RV, Too YC, Benito R, Stein W. Exergetic analysis of supercritical CO₂ Brayton cycles integrated with solar central receivers. *Appl. Energy* 2015;148:348-65.
- [18] Singh H, Mishra RS. Performance analysis of solar parabolic trough collectors driven combined supercritical CO₂ and organic Rankine cycle. *Eng. Sci. Technol.* 2018;21:451-64.
- [19] Chacartegui R, Sánchez D, Muñoz JM, Sánchez T. Alternative ORC bottoming cycles for combined cycle power plants. *Appl. Energy* 2009;86:2162-70.
- [20] Vignarooban K, Xu X, Arvay A, Hsu K, Kannan AM. Heat transfer fluids for concentrating solar power systems—a review. *Appl. Energy* 2015;146:383-96.
- [21] Freeman J, Guarracino I, Kalogirou SA, Markides CN. A small-scale solar organic Rankine cycle combined heat and power system with integrated thermal energy storage. *Appl. Therm. Eng.* 2017;127:1543-54.
- [22] Ramos A, Chatzopoulou MA, Freeman J, Markides CN. Optimisation of a high-efficiency solar-driven organic Rankine cycle for applications in the built environment. *Appl. Energy* 2018;228: 755-765.
- [23] Song J, Li XS, Ren XD, Gu CW. Performance analysis and parametric optimization of supercritical carbon dioxide (S-CO₂) cycle with bottoming organic Rankine cycle (ORC). *Energy* 2018;143:406-16.
- [24] Wang K, Pantaleo AM, Herrando M, Pasmazoglou, I, Franchetti BM., Markides CN. Thermoeconomic assessment of a spectral splitting hybrid PVT system in dairy farms for combined heat and power. In *Proc: 32nd Int. Conf. Effic. Cost Optim. Simul. Environ. Impact Energy Syst., Wroclaw, 2019.*
- [25] Song J, Li X, Wang K, Simpson M, Sapin P, Shu G, Tian H, Markides CN. Thermodynamic and economic comparison of organic Rankine cycle (ORC) and CO₂-cycle systems in internal combustion engine (ICE) waste-heat recovery applications. In *Proc: Sust. Therm. Energy Manag., Hangzhou, 2019.*
- [26] <https://solarpaces.nrel.gov/by-technology/parabolic-trough> (accessed 22 May, 2019)